JCTC Journal of Chemical Theory and Computation

Article

Cite This: J. Chem. Theory Comput. 2019, 15, 4170−4179

pubs.acs.org/JCTC

Benchmarks for Electronically Excited States with CASSCF Methods

Benjamin Helmich-Paris*

Max-Planck-Institut für Kohlenforschung, Kaiser-Wilhelm-Platz 1, D-45470 Mülheim an der Ruhr, Germany

Supporting Information

ABSTRACT: The accuracy of three different complete active space (CAS) self-consistent field (CASSCF) methods is investigated for the electronically excited-state benchmark set of Schreiber, M.; et al. *J. Chem. Phys.* **2008**, *128*, 134110. Comparison of the CASSCF linear response (LR) methods MC-RPA and MC-TDA and the state-averaged (SA) CASSCF method is made for 122 singlet excitation energies and 69 oscillator strengths. Of all CASSCF methods, when considering the complete test set, MC-RPA performs best for both excitation energies and oscillator strengths with a mean absolute error (MAE) of 0.74 eV and 51%, respectively. MC-TDA and SA-CASSCF show a similar accuracy for the excitation energies with a MAE of ∼1 eV with respect to more accurate coupled cluster (CC3) excitation energies. The opposite trend is observed for the subset of n → π^* excitation energies for which SA-CASSCF exhibits the least deviations (MAE 0.65 eV). By looking at *s*-tetrazine in more detail, we conclude that better performance for the n → π^* SA-CASSCF excitation energies can be attributed to a fortunate error compensation. For oscillator strengths, SA-CASSCF performs worst for the complete test set (MAE 100%) as well as for the subsets of n → π^* (MAE 192%) and π → π^* excitations (MAE 84.9%). In general, CASSCF gives the worst performance for excitation energies of all excited-state ab initio methods considered so far due to lacking the major part of dynamic electron correlation, though MC-RPA and TD-DFT (BP86) show similar performance. Among all LR-type methods, LR-CASSCF oscillator strengths are the ones with the least accuracy for the same reason. As state-specific orbital relaxation effects are accounted for in LR-CASSCF, oscillator strengths are significantly more accurate than those of MS-CASPT2. Our findings should encourage further developments of response theory-based multireference methods with higher accuracy and feasibility.

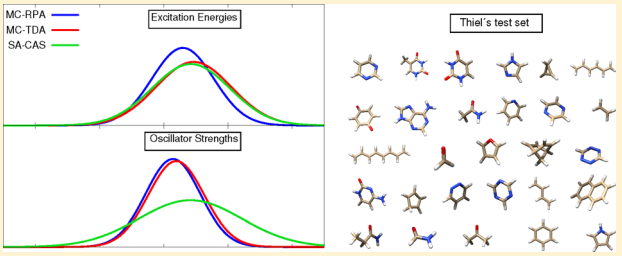

1. INTRODUCTION

In 2008, Schreiber et al. established a benchmark set of 28 closed-shell organic molecules that are intended to represent the most important classes of chromophors,[1] which is commonly referred to as Thiel's test set. The authors computed for those molecules in total 223 vertical singlet and triplet excitation energies and oscillator strengths of various π → π^*, n → π^*, and σ → π^* valence excitations. In the initial study, accurate ab initio methods like the complete active space (CAS) second-order perturbation theory method[2−4] (CASPT2) and a hierarchy of coupled cluster (CC) linear response (LR) methods CC2,[5] CCSD,[6,7] and CC3[8,9] were used. On the basis of their results[1,10,11] and on previously published literature data, best estimates for each excited state in the test set were proposed that served as reference values in later studies.

The same benchmark set has been employed in subsequent studies by many groups to assess the accuracy of a plethora of excited-state electronic structure methods that were not covered in Thiel's test set[1] originally. Silva-Junior et al.[12] reported time-dependent density functional theory (TD-DFT)[13,14] calculations with standard density functionals (BP86,[15,16] B3LYP,[15,17,18] and BHLYP[17,19]) as well as calculations with the semiempirical DFT-based multireference configuration interaction (DFT/MRCI) method.[20,21] The M06 family of density functionals[22−24] were employed by Jacquemin et al.,[25] while Maier et al.[26] used their newly developed local hybrid density functionals.[27,28] Moreover, excited-state calculations with the Bethe−Salpeter equation (BSE) starting from different Kohn−Sham DFT solutions were presented by Bruneval et al.[29,30] and Jacquemin et al.[31−33] Liu and Subotnik benchmarked their variationally optimized CI singles method.[34] Also, a variety of semiempirical methods for excited states were benchmarked by Silva-Junior and Thiel[35] and Gadaczek et al.[36] Recently, benchmark results for second-order perturbative polarization propagator (SOPPA) methods and the related algebraic diagrammatic construction (ADC) were published by several groups.[37−39] Scaled-opposite spin CC2 and ADC(2) benchmark results were reported by Winter and Hättig.[40] Kánnár and Szalay employed Thiel's benchmark set to compare CC oscillator strengths computed with LR theory[6,7] and the equation-of-motion[41,42] (EOM) ansatz.[43] Piecuch et al. employed their renormalized EOM-CC method when benchmarking Thiel's test set.[44] The similarity-transformed EOM-CC[45,46] calculations with many variants[47] were presented by Sous et al.[48] and Dutta et al.[49] Moreover, Hättig[39,50−52] and Neese[49] and their co-workers used Thiel's

Received: April 3, 2019
Published: May 28, 2019

DOI: 10.1021/acs.jctc.9b00325
J. Chem. Theory Comput. 2019, 15, 4170−4179

test set to investigate the accuracy of their reduced-scaling CC and ADC excited-state implementations that are based on pair natural orbitals.[50,53,54] Besides CASPT2, also other multireference wave function methods were employed for benchmarking excited states with Thiel's test set. Schapiro et al. reported state-specific (SS) second-order n-electron valence perturbation theory excitation energies.[55] Li et al. tested the accuracy of their driven similarity renormalization group method truncated to second order (DSRG-PT2) for singlet excitation energies.[107] Hubert et al.[56] and Hedegård[57] presented excitation energies and oscillator strengths for LR long-range MCSCF short-range DFT (srDFT) methods[58−60] that significantly improve the LR-CASSCF and TD-DFT results.

In the present study, we examine the accuracy of three different CASSCF methods for excited states. The first two variants are based on CASSCF LR theory for which the excitation energies and transition moments are obtained from the poles and residues of the CASSCF LR function,[61−63] also known as the polarization propagator.[64] This necessitates the solution of the generalized eigenvalue problem

$$\begin{pmatrix} \mathbf{A} & \mathbf{B} \\ \mathbf{B}^* & \mathbf{A}^* \end{pmatrix} \begin{pmatrix} \mathbf{Z} \\ \mathbf{Y}^* \end{pmatrix} = \omega \begin{pmatrix} \mathbf{\Sigma} & \mathbf{\Delta} \\ -\mathbf{\Delta}^* & -\mathbf{\Sigma}^* \end{pmatrix} \begin{pmatrix} \mathbf{Z} \\ \mathbf{Y}^* \end{pmatrix} \tag{1}$$

Solving the complete set of eq 1 is often referred to as the multiconfigurational random phase approximation (MC-RPA). When invoking the MC Tamm−Dancoff approximation (MC-TDA), the coupling blocks $\mathbf{B}$ and $\mathbf{\Delta}$ in eq 1 are omitted.

Conceptually, it is much simpler to determine excited-state CASSCF wave functions directly by enforcing convergence to a specific excited state than solving the CASSCF-LR eigenvalue eq 1. However, such a SS-CASSCF approach usually suffers from convergence problems that are caused by root flipping.[65] A much more convenient and computationally even simpler approach is state-averaged (SA) CASSCF, which performs a constrained minimization of a weighted sum over energies of multiple states.[65,66] Both ground- and excited-state wave functions are described within the SA approximation by SS CI coefficients but use a global single set of orbitals. Beside the two LR-CASSCF variants MC-RPA and MC-TDA, we also consider the SA-CASSCF method in the present benchmark study.

Despite its tempting simplicity, SA-CASSCF has a couple of drawbacks: (i) Excitation energies and oscillator strengths are dependent on the number of states and their corresponding weight for the averaging. (ii) It is not possible to describe electronic excitations out of the active model space. This often requires large active spaces for the full CAS-CI calculation. In such situations CAS-CI is—if at all—only affordable with state-of-the-art quantum Monte Carlo,[67,68] selected CI,[69−74] or density matrix renormalization group[75−84] algorithms. (iii) If many roots are optimized simultaneously, valence and Rydberg states with the same symmetry tend to mix. This unphysical behavior inherent of SA-CASSCF must be cured a posteriori by multistate variants of MRPT[4,85−87] or MRCC.[88]

LR-CASSCF does not suffer from all these of issues and should in general be preferred over SA-CASSCF. Moreover, due to the presence of both orbital rotation parameters and state transfer CI coefficients[89] in the response vectors, LR-CASSCF provides SS orbital relaxation, which is missing in SA-CASSCF. Another advantage of the full LR-CASSCF method (MC-RPA) is that a minor fraction of dynamic difference electron correlation is also captured as for all RPA-type methods.[90] Nevertheless, SA-CASSCF has its merits in the case of quasi-degenerate ground-state wave functions, which is, for the time being, still a problem for response theory methods.

It is noted in passing that all three CASSCF variants for excited states give numerically identical results in the limit of a FCI calculation, i.e., all orbitals are included in the CAS-CI calculation.

The computational costs of LR-CASSCF calculations are comparable to those of SA-CASSCF if only a few states are computed. If the orbital part in a CASSCF calculation (not the CAS-CI problem) has the largest contribution to the timings and the number of requested states is large, SA-CASSCF will eventually be more efficient than LR-CASSCF. Still, LR-CASSCF calculations of large open-shell molecules with hundreds of atoms are now feasible[91] assuming that the CAS is of moderate size and the CAS-CI calculation is affordable.

Even though both excited-state CASSCF methods have been available for more than 4 decades, a systematic comparison and error analysis for excitation energies and oscillator strengths has not been attempted so far. A benchmark study on the accuracy of SA- and LR-CASSCF is particularly interesting because SA-CASSCF is used more frequently in practice, though—following the discussion above—LR-CASSCF seems to be advantageous in many aspects. For this purpose, we employ in the present study Thiel's test set as it contains highly accurate reference data obtained from CC3 calculations.[1,43] Furthermore, we compare the errors of CASSCF with those of several other excited-state methods that were employed in previous benchmark studies. The accuracy of CC3 has been confirmed very recently by Loos et al. for a test set of 18 small molecules and amounts to a mean absolute error (MAE) of 0.03 eV in comparison to extrapolated selected full CI (FCI) calculations.[92] It should be noted at this point that the target application of CASSCF methods in electronic spectroscopy are open-shell molecules with multireference character primarily. Unfortunately, neither Thiel's test set nor any other published excited-state test set contains open-shell low-spin systems for which highly accurate MRCC or approximated FCI methods were employed as reference; however, benchmark studies on high-spin open-shell systems have been published recently.[93−95]

The article on our CASSCF benchmark study is organized as follows: In section 2, we provide details on the calculations and on the data processing for the statistical analysis. In section 3, CASSCF calculations for singlet excitation energies and oscillator strengths are presented, and their deviations from CC3 references are discussed. We also compare errors of CASSCF with the ones of other excited-state methods. In the final section 4, we summarize our findings and give recommendations for future developments.

2. COMPUTATIONAL DETAILS

All SA-[96] and LR-CASSCF[91] calculations were performed with the ORCA quantum chemistry package version 4.1.1.[97] The ground-state equilibrium geometries of the 28 organic molecules were taken from the original test set[1,43] for reasons of comparability. For the same reason, we employed the TZVP[98] and aug-cc-pVTZ[99] basis set for all calculations. The resolution-of-the-identity (RI) approximation was used throughout for the two-electron integrals with three and four active indices.[96] The corresponding def2/JK[100] and aug-cc-pVTZ[101] auxiliary basis set was chosen for the RI

DOI: 10.1021/acs.jctc.9b00325
J. Chem. Theory Comput. 2019, 15, 4170−4179

approximation with the Coulomb metric,[102] respectively. The $1s^2$ core electrons of the C, N, and O atoms were kept frozen for all LR-CASSCF calculations.

Different choices of active spaces had to be made depending on the type of CASSCF calculation, i.e. either LR- or SA-CASSCF, for the following reason. Prior to the LR calculation, a SS-CASSCF calculation was performed for the lowest totally symmetric singlet state. It turned out that such energy optimizations become unfeasible due to numerical difficulties if almost doubly occupied, e.g., sigma or nonbonding orbitals, are included in the active space. If not otherwise noted, the default active space for LR-CASSCF calculations comprises of only valence π and π^* orbitals. One additional spectator orbital had to be added to the default active space of the three amides to ensure that all π and π^* orbitals are held in the CAS in the course of the SS-CASSCF energy minimization. For all SA-CASSCF calculations, the original active space of ref 1 was employed, which may also comprise nonbonding and sigma orbitals to describe n $\rightarrow \pi^*$ and $\sigma \rightarrow \pi^*$ excitations. Note that in a π-only LR-CASSCF calculation those transitions are primarily described by the orbital rotation part of the response vectors.

To make a fair comparison between LR- and SA-CASSCF, as few as possible states were considered in the state averaging. The number of states per point group *irrep*, along with the symmetry group exploited in the calculation and the number of active orbitals and electrons in the CAS, is provided in Tables 1 and 2 of the Supporting Information for calculations with the TZVP and aug-cc-pVTZ basis sets, respectively. In contrast to previous works,[1,55] we average over all singlet states even if they belong to different *irreps* because for technical reasons a single set of orthogonal orbitals is required for computing the transition moments with SA-CASSCF in ORCA. In many cases, fewer states were included in the SA in comparison with refs 1 and 55 as we are not facing MRPT-specific intruder-state problems.

Apart from comparing LR- and SA-CASSCF transition moments, an assignment of the electronic excitations between those methods was made by visualizing natural transition orbitals[91,103] (NTOs) and active natural orbitals, respectively. To relate our results to those of ref 1, NTOs of the CC2 excited states that form part of the original test set[1] were inspected whenever necessary.

3. RESULTS AND DISCUSSION

3.1. Excitation Energies. Singlet excitation energies were computed with MC-RPA, MC-TDA, and SA-CASSCF for a subset of the original benchmark set of ref 1, which in the present study comprises 122 $\pi \rightarrow \pi^*$, n $\rightarrow \pi^*$, and $\sigma \rightarrow \pi^*$ excitations for the TZVP basis set altogether. Concerning the aug-cc-pVTZ basis set results, we investigated only those 23 states for which accurate CC3/aug-cc-pVTZ reference excitation energies were provided in a previous study.[10] These excitation energies are compiled in Tables 3 and 4 in the Supporting Information for the TZVP and aug-cc-pVTZ basis set, respectively, along with the accurate CC3 and MS-CASPT2 results taken from the literature.[1,10,11,43] We decided to include only those states in our study for which a clear assignment between different electronic structure methods could be made and that have been investigated with all other excited-state methods that we compare with, i.e., CC2,[1] CCSD,[1] MS-CASPT2,[1] SS-NEVPT2,[55] CAS-srPBE,[56,57] ADC(2),[38] ADC(3),[38] BP86,[12] B3-LYP,[12] and the BSE.[32] As the number of CC3/aug-cc-pVTZ reference excitation energies available from ref 10 is much smaller (23) than those of CC3/TZVP (122), we decided to omit the statistical analysis for the aug-cc-pVTZ basis set also because most other excited-state benchmark studies used the TZVP basis set.

Statistical measures on the deviation with respect to CC3 reference excitation energies are given in Table 1. Though redundant, the normal distribution of those deviations is plotted in Figure 1 for illustrative purposes. All excitation energies with the LR- and SA-CASSCF variants are on average systematically blue shifted. Concerning the whole test set and the subset of $\pi \rightarrow \pi^*$ excitations, MC-RPA gives on average the least deviation from the reference. The largest outlier MAX(+) for MC-RPA and MC-TDA is the 2 $^1B_{2g}$ state in *s*-tetrazine, which we discuss later. The superior (statistical) performance of the full LR-CASSCF (MC-RPA) could have been anticipated because the rotation of orbitals when exciting from the ground to an excited state is incorporated into the orbital-rotation part of the LR eigenvectors. On the contrary, SA-CASSCF uses a single set of orbitals for both the ground state and all excited states. Thus, any kind of SS orbital relaxation effects are ignored in the SA-CASSCF method. Moreover, the statistical analysis reveals that applying the TDA deteriorates the accuracy of LR-CASSCF noticeably. According to the variational principle, the lowest excitation energy for each *irrep* is always strictly larger when invoking the TDA. By comparing each MC-RPA and MC-TDA excitation energy in Table 3 of the Supporting Information, we can see that even for the higher roots MC-RPA excitation energies are lower than those of MC-TDA except for the 2 $^1B_{1g}$ state in pyrazine. Because the MC-RPA excitation energies are on average

Table 1. Statistical Analysis of the Singlet CASSCF Excitation Energy Deviation with Respect to a CC3 Reference Given in eV[a]

	MC-RPA	MC-TDA	SA-CAS
complete test set			
count	122	122	122
ME	0.63	0.96	0.84
MAE	0.74	1.01	0.98
SD	0.78	0.73	0.87
MAX(+)	3.57	3.63	3.09
MAX(−)	−0.74	−0.43	−0.85
n $\rightarrow \pi^*$ subset			
count	39	39	39
ME	0.98	1.46	0.40
MAE	1.02	1.46	0.65
SD	1.02	0.80	0.84
MAX(+)	3.57	3.63	3.09
MAX(−)	−0.25	0.37	−0.85
$\pi \rightarrow \pi^*$ subset			
count	80	80	80
ME	0.47	0.74	1.08
MAE	0.62	0.81	1.16
SD	0.58	0.58	0.82
MAX(+)	2.81	3.04	2.50
MAX(−)	−0.74	−0.43	−0.56

[a]The following abbreviations were used: ME — mean error; MAE — mean absolute error; SD — standard deviation; MAX(+) — maximum error with positive sign; MAX(−) — maximum error with negative sign.

DOI: 10.1021/acs.jctc.9b00325
J. Chem. Theory Comput. 2019, 15, 4170−4179

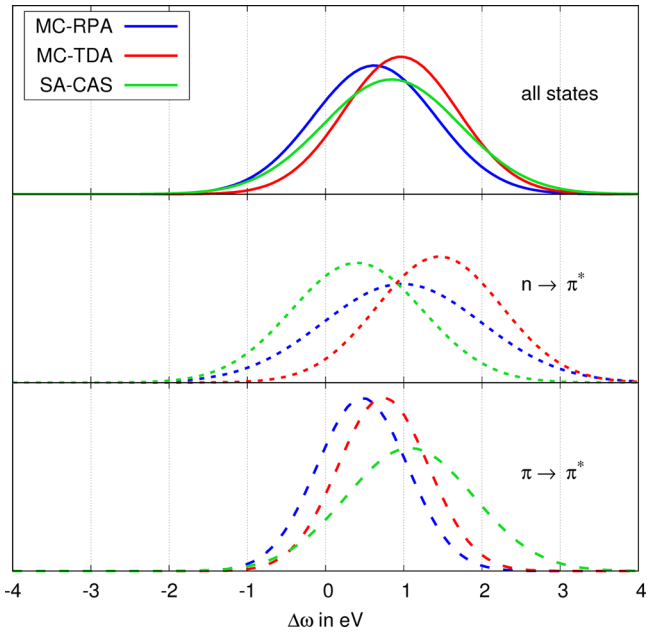

Figure 1. Normal distribution of deviation from the CC3 reference singlet excitation energies of the complete test set and subsets of n → π^* and $\pi \rightarrow \pi^*$ excitations.

already blue shifted, the mean deviation of MC-TDA with respect to the reference is increased. It was shown in a previous work on an efficient LR-CASSCF implementation[91] that the computational performance is improved only marginally when invoking the TDA even though there are fewer terms due to the neglect of coupling blocks in eq 1. Due to the higher accuracy of MC-RPA, we conclude that employing the TDA should in general be omitted for LR-CASSCF excitation energy calculations.

For the subset of n → π^* excitations, the SA-CASSCF excitation energies show much smaller deviations from the reference than LR-CASSCF for which a π-only active space is employed. For those n → π^* excitations, all relevant nonbonding orbitals at the N and O atoms that are involved in the excitation processes are also included in the active space of SA-CASSCF calculations. Additional dynamic difference correlation is accounted for in n → π^* excitations in SA-CASSCF calculations by means of an enlarged active space that is augmented by the relevant nonbonding orbitals. By contrast, the n → π^* LR eigenvectors are expanded primarily in terms of orbital rotation parameters, and a major part of electron correlation is missing. Hence, LR-CASSCF is outperformed by SA-CASSCF for the n → π^* excitations with the current choice of active spaces, as shown in Table 1 and Figure 1.

At this point, we would like to investigate if and how an augmented active space affects the accuracy of LR-CASSCF excitations, primarily for n → π^* excitations. For this purpose, we compare the lowest CC3 and CASSCF excitation energies of *s*-tetrazine with two different active spaces in Figure 2. Employing the augmented CAS(14,10) lowers systematically the deviation from CC3 compared to the π-only active space for all of the nine lowest states of *s*-tetrazine. However, the difference of the CAS(14,10) and CAS(6,6) LR-CASSCF excitation energies varies strongly among the nine lowest states. In the case of the 1 $^1B_{3u}$ state, the MC-RPA and MC-TDA excitation energies are only lowered when augmenting the active space by −0.037 and −0.147 eV, respectively. In

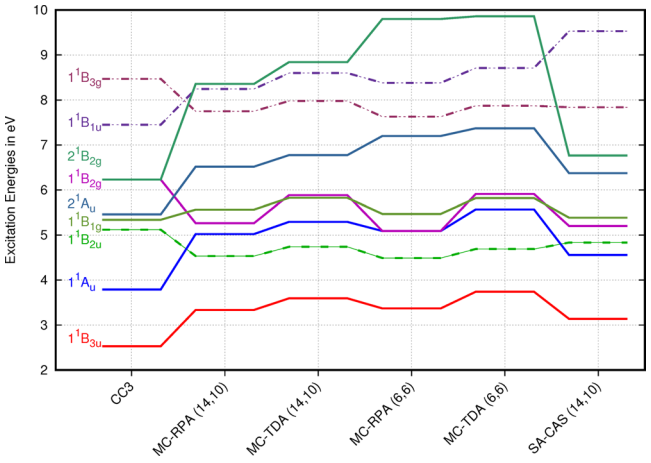

Figure 2. Lowest singlet excitation energies of *s*-tetrazine with different CASSCF methods and CC3. Solid lines are n → π^* excitations; dashed lines are $\pi \rightarrow \pi^*$ excitations.

contrast to this, the MC-RPA and MC-TDA excitation energies of 2 $^1B_{2g}$ improve significantly in accuracy with CAS(14,10) by −1.441 and −1.018 eV, respectively. That is surprising as 1 $^1B_{3u}$ and 2 $^1B_{2g}$ are both n → π^* excitations and should in principal benefit from an augmented active space in the LR-CASSCF calculation. From all CASSCF excited-state variants discussed here, the SA-CASSCF shows the best agreement with accurate CC3 reference data, which is in line with the average performance for the subset of n → π^* excitations. This is mainly caused by cancellation of errors in the SA approximation for which the ground-state energy increases more than the excited-state energies. This may partially compensate the lack of differential dynamic correlation, which usually lowers excitation energies. The fortunate error compensation of SA-CASSCF can be revealed when computing excitation energies with the SS-CASSCF approach. The deviation of SS-CASSCF from the CC3 reference for the 1 $^1B_{3u}$ state is by 3.51 eV much larger than the deviation of SA-CASSCF (3.14 eV) and MC-RPA (3.37 eV CAS(6,6); 3.34 eV CAS(14,10)).

It has been discussed already in section 2 that adding strongly occupied orbitals to the active space usually results in convergence issues of the SS CASSCF energy minimization. Instead of extending the active space, dynamic correlation effects on excitation energies and transition properties should rather taken into account by MRPT[104] or MRCC-based[105] LR methods, which are at the moment not fully explored yet and available in terms of pilot implementations or from automatically generated codes. Alternatively, dynamic correlation can be introduced by means of exchange−correlation functionals in a very cost-effective fashion, as shown for srDFT-type methods.[56−60]

To compare the accuracy of CASSCF with other excited-state methods, we performed a statistical analysis for exactly the same states as those in Thiel's test set that were computed in previous works with CC2,[1] CCSD,[1] MS-CASPT2,[1] SS-NEVPT2,[55] CAS-srPBE,[56,57] ADC(2),[38] ADC(3),[38] BP86,[12] and B3-LYP.[12] The statistical measures are compiled in Table 3. The normal distribution for some of the just mentioned excited-state methods is shown in Figure 3. It is interesting to see that MC-RPA (MAE = 0.74 eV) excitation energies show statistically a similar (but slightly worse) performance as BP86 (TD-DFT, MAE = 0.67 eV); however, MC-RPA excitation

DOI: 10.1021/acs.jctc.9b00325
J. Chem. Theory Comput. 2019, 15, 4170−4179

Table 2. Statistical Analysis of CASSCF Oscillator Strengths[a]

	MC-RPA	MC-TDA	SA-CAS
complete test set			
count	69	69	69
ME	25.8	33.8	79.0
MAE	50.8	55.7	100.
SD	79.3	76.7	134.
MAX(+)	469.	366.	870.
MAX(−)	−89.7	−86.8	−95.5
n → π^* subset			
count	10	10	10
ME	71.4	114.	184.
MAE	91.4	131.	192.
SD	77.9	97.5	252.
MAX(+)	153.	227.	870.
MAX(−)	−85.0	−85.3	−35.9
$\pi \rightarrow \pi^*$ subset			
count	59	59	59
ME	18.1	20.2	61.1
MAE	43.9	42.9	84.9
SD	77.5	64.3	93.9
MAX(+)	469.	366.	341.
MAX(−)	−89.7	−86.8	−95.5

[a]Only those states with $f > 0.003$ were included in the analysis. Relative deviations with respect to CC3 are given in percent. The following abbreviations were used: ME — mean error; MAE — mean absolute error; SD — standard deviation; MAX(+) — maximum error with positive sign; MAX(−) — maximum error with negative sign.

energies are on average blue shifted, whereas the ones of BP86 are shifted into the red. As has been pointed out already by Hubert et al.[56] and Hedegård,[57] a combination of MC-RPA and TD-DFT by means of the srDFT ansatz significantly improves the accuracy (MAE = 0.26 eV), which is comparable to the MRPT methods MS-CASPT2 (MAE = 0.21 eV) and SS-NEVPT2 (MAE = 0.22 eV). Also ADC(2) and ADC(3) show on average a similar accuracy as CAS-srPBE (see Table 3). The smallest errors were obtained from the CC LR methods CCSD (MAE = 0.24 eV, SD = 0.17 eV) and CC2 (MAE = 0.13 eV, SD = 0.19 eV).

3.2. Oscillator Strengths. Accurate CC3 oscillator strengths f were omitted in the initial work of Schreiber et al.[1] but have been provided some years later by Kánnár and Szalay[43] for the TZVP basis set with the purpose to compare LR- and EOM-CC oscillator strengths. Those CC3/TZVP oscillator strengths are taken as reference in the present work when benchmarking the SA- and LR-CASSCF methods for

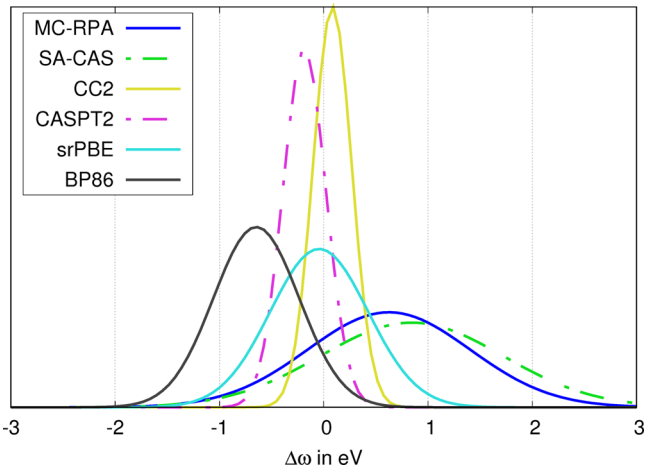

Figure 3. Normal distribution of deviation from the CC3 reference singlet excitation energies computed with various methods.

excited states. In the present study, we discuss only benchmark results with the TZVP basis set because accurate CC3/aug-cc-pVTZ oscillator strengths have not been reported so far for Thiel's test set. Because oscillator strengths of $\pi \rightarrow \pi^*$ excitations might be many orders of magnitude larger than those of n → π^* excitations, Kánnár and Szalay[43] suggested considering relative deviation from CC3 rather than absolute deviations as done for the excitation energies. However, this would lead to the situation that the error statistics are dominated by deviations of oscillator strengths that are small in magnitude, i.e., $\sigma \rightarrow \pi^*$ and n → π^* excitations. Therefore, only states with $f > 0.003$ are taken here into account for the statistical analysis, as done in previous investigations.[37]

Statistical measures on the deviation with respect to CC3 oscillator strengths are given in Table 2. For illustrative purposes, we plotted the normal distribution of those deviations in Figure 4. As can be seen in Table 2, MC-RPA has the lowest mean error (ME) and MAE for the complete set and the subsets of $\pi \rightarrow \pi^*$ and n → π^* excitations. Slightly larger ME and MAE are obtained when invoking the MC-TDA. Of the three methods covered in this work, SA-CASSCF shows the largest ME and MAE, which are larger than those of MC-RPA by roughly a factor of 1.2 to 3.2, respectively. Depending on the benchmark set, the standard deviation (SD) of SA-CASSCF from the CC3 references is by a factor of 2−3 larger than the SD of MC-RPA. Surprisingly, we observe one of the largest outliers (MAX (+)) for a MC-RPA $\pi \rightarrow \pi^*$ excitation, which gives on average the best performance for both singlet excitation energies and oscillator strengths. It is the 1 $^1B_2$ state in norbornadiene that also showed a significant

Table 3. Statistical Analysis of the Singlet Excitation Energy Deviation of Various Methods with Respect to a CC3 Reference Given in eV[a]

	CC2	CCSD	CASPT2	NEVPT2	srPBE	ADC(2)	ADC(3)	BP86	B3-LYP
count	122	122	122	122	122	122	122	122	122
ME	0.08	0.24	−0.19	0.01	−0.04	−0.08	−0.16	−0.65	−0.306
MAE	0.13	0.24	0.21	0.22	0.26	0.22	0.26	0.67	0.37
SD	0.19	0.17	0.21	0.30	0.47	0.47	0.44	0.41	0.325
MAX(+)	0.95	1.00	0.65	0.54	0.92	1.00	0.64	0.34	0.48
MAX(−)	−0.25	−0.31	−1.14	−1.37	−2.42	−2.96	−2.42	−1.90	−1.28

[a]The following abbreviations were used: ME — mean error; MAE — mean absolute error; SD — standard deviation; MAX(+) — maximum error with positive sign; MAX(−) — maximum error with negative sign.

DOI: 10.1021/acs.jctc.9b00325
J. Chem. Theory Comput. 2019, 15, 4170−4179

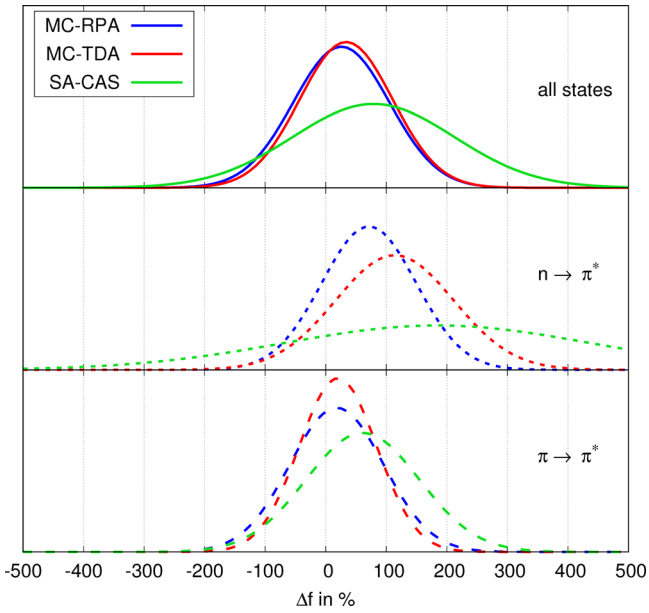

Figure 4. Normal distribution of deviation from the CC3 reference oscillator strengths of the complete test set and subsets of n → π^* and π → π^* excitations.

deviation in the excitation energy from CC3 of at least 1.39 eV. Apparently, a large part of the dynamic correlation contribution to the 1 $^1B_2$ excitation energy and transition moments is not included by any of the CASSCF methods. It is also interesting to see that for the oscillator strengths, on average, LR-CASSCF clearly outperforms SA-CASSCF also for the n → π^* excitations for which SA-CASSCF excitation energies performed best. This is a further indication for the importance of excited-state orbital relaxation covered by the LR-CASSCF method but omitted in SA-CASSCF.

At this point, we would like to investigate how the accuracy of CASSCF oscillator strengths compares with the one obtained from other excited-state methods. For this purpose, we have performed a statistical analysis of the oscillator strengths deviations from CC3 (see Table 4) that were computed from previously published results of CC2,[1] CCSD,[1] MS-CASPT2,[1] CAS-srPBE,[56,57] ADC(2),[38] ADC(3),[38] BP86,[12] B3-LYP,[12] and BSE[32] and have plotted the normal error distribution for some of the just mentioned methods in Figure 5. As for the singlet excitation energies, we observe that MC-RPA overshoots the oscillator strengths (ME = 25.8%), whereas BP86 (TD-DFT) underestimates them (ME = −18.2%). Again, a combination of MC-RPA with TD-DFT, i.e., srDFT, improves the accuracy of oscillator strengths (ME = 14.0%, SD = 44.0%), which is comparable to ADC(2), ADC(3), and BSE (see Table 4). As for singlet excitation energies, the oscillator strengths of CC LR variants CC2 (ME = 12.4%, SD = 19.6%) and CCSD (ME = 11.0%, SD = 15.0%) are the most accurate ones among the excited-state methods considered here.

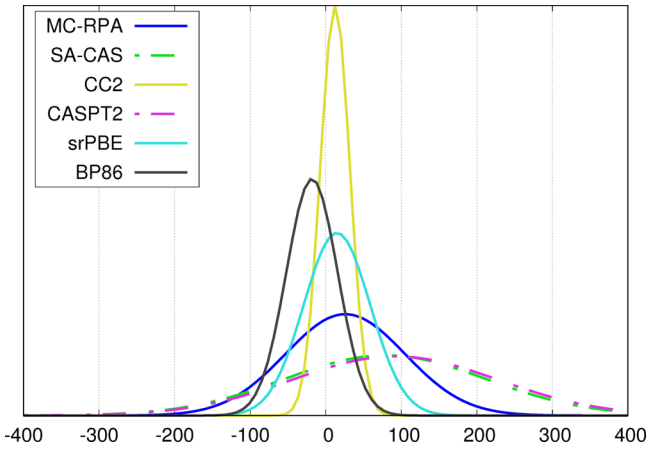

Figure 5. Normal distribution of deviation from the CC3 reference oscillator strengths computed with various methods.

In contrast to excitation energies, MS-CASPT2 shows the worst performance for oscillator strengths of all excited-state methods considered here. The already deficient accuracy of SA-CASSCF oscillator strengths is even degraded when considering the statistical measures in Table 4. Computing the transition moments from the one-particle density matrix that includes the first-order MRPT wave function might be more accurate than the perturbation modified CAS approximation[4,106] and could be explored in future MS-MRPT developments as implemented for the DSRG-PT2 method.[107]

4. CONCLUSIONS

The accuracy of SA-CASSCF and LR-CASSCF singlet excitation energies and oscillator strengths was investigated for the electronically excited-state benchmark set of Schreiber et al.,[1] which contains various valence $\pi \rightarrow \pi^*$, n → π^*, and $\sigma \rightarrow \pi^*$ excitations in 28 closed-shell organic molecules. For those states, highly accurate benchmark data from the CC3 method were provided,[1,43] which allows us to provide reliable statistical measures for more approximate electronic structure methods as CASSCF. Besides the full LR-CASSCF method, we have also investigated the accuracy of the Tamm−Dancoff approximation, which we refer to as MC-TDA.

For a set of 122 excited states, we showed that MC-RPA performs best with a MAE of 0.74 eV and a SD of 0.78 eV for

Table 4. Statistical Analysis of Oscillator Strengths from Various Methods[a]

	CC2	CCSD	CASPT2	srPBE	ADC(2)	ADC(3)	BP86	B3-LYP	BSE
count	69	69	69	69	69	69	69	69	69
ME	12.4	11.0	91.6	14.9	17.2	0.71	−18.2	−7.28	6.52
MAE	15.1	13.9	97.6	26.8	27.4	27.7	31.3	26.9	23.4
SD	19.6	15.0	136.	44.0	35.4	40.5	34.0	35.9	43.1
MAX(+)	120.0	60.0	858.	164.	140.	172.	78.9	97.4	176.
MAX(−)	−25.0	−50.0	−80.0	−75.1	−100.0	−100.0	−83.3	−83.3	−100.0

[a]Only those states with f > 0.003 were included in the analysis. Relative deviations with respect to CC3 are given in percent. The following abbreviations were used: ME — mean error; MAE — mean absolute error; SD — standard deviation; MAX(+) — maximum error with positive sign; MAX(−) — maximum error with negative sign.

DOI: 10.1021/acs.jctc.9b00325
J. Chem. Theory Comput. 2019, 15, 4170−4179

excitation energies. MC-TDA (MAE 1.01 eV and SD 0.73 eV) and SA-CASSCF (MAE 0.98 eV and SD 0.87 eV) showed on average larger errors with very similar statistical error measures. The accuracy of CASSCF excitation energies differs strongly for different types of excitations. The subset of $\pi \rightarrow \pi^*$ excitations was calculated significantly more accurately by the two CASSCF-LR methods with a MAE and SD that are up to a factor of 2 smaller than those with SA-CASSCF. By contrast, the average errors of CASSCF-LR are much larger than those of SA-CASSCF for the subset of $n \rightarrow \pi^*$ excitations. This has been attributed, on the one hand, to the larger active space for our SA-CASSCF calculations with nonbonding orbitals included and, on the other hand, to a fortunate error compensation for SA-CASSCF excitation energies in general.

In comparison with other excited-state methods that were previously used when studying Thiel's test set, CASSCF shows in general the worst performance for singlet excitation energies. A significant improvement of the accuracy with only minor computational overhead can be achieved with srDFT LR methods, which has been shown previously by Hubert et al.[56] and Hedegård.[57]

The statistical analysis for the CASSCF oscillator strength deviations from CC3 gave a more uniform picture than that for the singlet excitation energies. Among those three CASSCF methods, the two CASSCF-LR variants clearly outperform SA-CASSCF in terms of all statistical measures by often a factor of 2 and more for the whole test set as well as for the subsets of $\pi \rightarrow \pi^*$ and $n \rightarrow \pi^*$ excitations. Again, the full MC-RPA is on average more accurate than MC-TDA. When comparing MC-RPA oscillator strengths with other excited-state methods, we have shown that MC-RPA has the least accuracy of all LR-type methods. Again, including dynamic correlation as done in srDFT gives more accurate oscillator strengths than with BP86 (TD-DFT) and MC-RPA. By far, the least accurate oscillator strengths of all methods considered here were obtained by SA-CASSCF and MS-CASPT2.

From our point of view, the better performance of LR-CASSCF is mainly due to excited SS orbital relaxation mimicked by the orbital rotation part of the response vectors, which is omitted in SA-CASSCF (and MS-CASPT2) by construction. This is revealed especially when comparing the accuracy of oscillator strength calculations with SA- and LR-CASSCF that are also sensitive to errors in the ground- and excited-state wave functions rather in energies.

Our results should encourage further developments in the field of MR-LR or MR polarization propagator methods that also account for the majority of dynamic correlation effects, as has been initiated recently.[104] It would also be interesting and much needed to assess the accuracy of excitation energies and excited-state properties calculated from CASSCF and other multireference methods for open-shell molecules, in particular, transition metal complexes in a low-spin state. Such an endeavor has not been undertaken so far due to the lack of highly accurate and, at the same time, computationally feasible MR methods. This may change in the future with more efficient selected FCI or MRCC implementations.

■ ASSOCIATED CONTENT

Supporting Information

The Supporting Information is available free of charge on the ACS Publications website at DOI: 10.1021/acs.jctc.9b00325.

Number of states for each *irrep* employed in the SA-CASSCF TZVP and aug-cc-pVTZ calculations and all MC-RPA, MC-TDA, and SA-CASSCF excitation energies (TZVP and aug-cc-pVTZ) and oscillator strengths (TZVP) together with the CC3 and MS-CASPT2 results (PDF)

■ AUTHOR INFORMATION

Corresponding Author

*E-mail: helmichparis@kofo.mpg.de.

ORCID

Benjamin Helmich-Paris: 0000-0002-3616-9671

Funding

The author acknowledges gratefully financial support from The Netherlands Organisation for Scientific Research NWO by a Veni fellowship (Grant No. 722.016.011).

Notes

The author declares no competing financial interest.

■ ACKNOWLEDGMENTS

The author thanks cordially Frank Neese, Alexander A. Auer, Róbert Izsák, and Kantharuban Sivalingam for fruitful scientific discussions.

■ REFERENCES

(1) Schreiber, M.; Silva-Junior, M. R.; Sauer, S. P. A.; Thiel, W. Benchmarks for electronically excited states: CASPT2, CC2, CCSD, and CC3. *J. Chem. Phys.* **2008**, *128*, 134110.

(2) Andersson, K.; Malmqvist, P. Å.; Roos, B. O.; Sadlej, A. J.; Wolinski, K. Second-order perturbation theory with a CASSCF reference function. *J. Phys. Chem.* **1990**, *94*, 5483−5488.

(3) Andersson, K.; Malmqvist, P.-Å.; Roos, B. O. Second-order perturbation theory with a complete active space self-consistent field reference function. *J. Chem. Phys.* **1992**, *96*, 1218−1226.

(4) Finley, J.; Malmqvist, P.-Å.; Roos, B. O.; Serrano-Andrés, L. The multi-state CASPT2 method. *Chem. Phys. Lett.* **1998**, *288*, 299−306.

(5) Christiansen, O.; Koch, H.; Jørgensen, P. The second-order approximate coupled cluster singles and doubles model CC2. *Chem. Phys. Lett.* **1995**, *243*, 409−418.

(6) Koch, H.; Jørgensen, P. Coupled cluster response functions. *J. Chem. Phys.* **1990**, *93*, 3333−3344.

(7) Koch, H.; Jensen, H. J. A.; Jørgensen, P.; Helgaker, T. Excitation-energies from the coupled cluster singles and doubles linear response function (CCSDLR). Applications to Be, CH^+, CO, and H_2O. *J. Chem. Phys.* **1990**, *93*, 3345−3350.

(8) Christiansen, O.; Koch, H.; Jørgensen, P. Response functions in the CC3 iterative triple excitation model. *J. Chem. Phys.* **1995**, *103*, 7429−7441.

(9) Koch, H.; Christiansen, O.; Jørgensen, P.; Sanchez de Merás, A. M.; Helgaker, T. The CC3 model: An iterative coupled cluster approach including connected triples. *J. Chem. Phys.* **1997**, *106*, 1808−1818.

(10) Silva-Junior, M. R.; Sauer, S. P.; Schreiber, M.; Thiel, W. Basis set effects on coupled cluster benchmarks of electronically excited states: CC3, CCSDR(3) and CC2. *Mol. Phys.* **2010**, *108*, 453−465.

(11) Silva-Junior, M. R.; Schreiber, M.; Sauer, S. P. A.; Thiel, W. Benchmarks of electronically excited states: Basis set effects on CASPT2 results. *J. Chem. Phys.* **2010**, *133*, 174318.

(12) Silva-Junior, M. R.; Schreiber, M.; Sauer, S. P. A.; Thiel, W. Benchmarks for electronically excited states: Time-dependent density functional theory and density functional theory based multireference configuration interaction. *J. Chem. Phys.* **2008**, *129*, 104103.

(13) Runge, E.; Gross, E. K. U. Density-functional theory for time-dependent systems. *Phys. Rev. Lett.* **1984**, *52*, 997−1000.

(14) Gross, E.; Kohn, W. In *Density functional theory of many-fermion systems*; Löwdin, P.-O., Ed.; Advances in Quantum Chemistry; Academic Press, 1990; Vol. *21*; pp 255−291.
(15) Becke, A. D. Density-functional exchange-energy approximation with correct asymptotic behavior. *Phys. Rev. A: At., Mol., Opt. Phys.* **1988**, *38*, 3098−3100.
(16) Perdew, J. P. Density-functional approximation for the correlation energy of the inhomogeneous electron gas. *Phys. Rev. B: Condens. Matter Mater. Phys.* **1986**, *33*, 8822−8824.
(17) Lee, C.; Yang, W.; Parr, R. G. Development of the Colle-Salvetti correlation-energy formula into a functional of the electron density. *Phys. Rev. B: Condens. Matter Mater. Phys.* **1988**, *37*, 785−789.
(18) Becke, A. D. Density-functional thermochemistry. III. The role of exact exchange. *J. Chem. Phys.* **1993**, *98*, 5648−5652.
(19) Becke, A. D. A new mixing of Hartree-Fock and local density-functional theories. *J. Chem. Phys.* **1993**, *98*, 1372−1377.
(20) Grimme, S. Density functional calculations with configuration interaction for the excited states of molecules. *Chem. Phys. Lett.* **1996**, *259*, 128−137.
(21) Grimme, S.; Waletzke, M. A combination of Kohn-Sham density functional theory and multi-reference configuration interaction methods. *J. Chem. Phys.* **1999**, *111*, 5645−5655.
(22) Zhao, Y.; Truhlar, D. G. A new local density functional for main-group thermochemistry, transition metal bonding, thermochemical kinetics, and noncovalent interactions. *J. Chem. Phys.* **2006**, *125*, 194101.
(23) Zhao, Y.; Truhlar, D. G. Density Functional for Spectroscopy: No Long-Range Self-Interaction Error, Good Performance for Rydberg and Charge-Transfer States, and Better Performance on Average than B3LYP for Ground States. *J. Phys. Chem. A* **2006**, *110*, 13126−13130.
(24) Zhao, Y.; Truhlar, D. G. Density Functionals with Broad Applicability in Chemistry. *Acc. Chem. Res.* **2008**, *41*, 157−167.
(25) Jacquemin, D.; Perpète, E. A.; Ciofini, I.; Adamo, C.; Valero, R.; Zhao, Y.; Truhlar, D. G. On the Performances of the M06 Family of Density Functionals for Electronic Excitation Energies. *J. Chem. Theory Comput.* **2010**, *6*, 2071−2085.
(26) Maier, T. M.; Bahmann, H.; Arbuznikov, A. V.; Kaupp, M. Validation of local hybrid functionals for TDDFT calculations of electronic excitation energies. *J. Chem. Phys.* **2016**, *144*, 074106.
(27) Bahmann, H.; Kaupp, M. Efficient Self-Consistent Implementation of Local Hybrid Functionals. *J. Chem. Theory Comput.* **2015**, *11*, 1540−1548.
(28) Maier, T. M.; Bahmann, H.; Kaupp, M. Efficient Semi-numerical Implementation of Global and Local Hybrid Functionals for Time-Dependent Density Functional Theory. *J. Chem. Theory Comput.* **2015**, *11*, 4226−4237.
(29) Bruneval, F.; Hamed, S. M.; Neaton, J. B. A systematic benchmark of the ab initio Bethe-Salpeter equation approach for low-lying optical excitations of small organic molecules. *J. Chem. Phys.* **2015**, *142*, 244101.
(30) Rangel, T.; Hamed, S. M.; Bruneval, F.; Neaton, J. B. An assessment of low-lying excitation energies and triplet instabilities of organic molecules with an ab initio Bethe-Salpeter equation approach and the Tamm-Dancoff approximation. *J. Chem. Phys.* **2017**, *146*, 194108.
(31) Jacquemin, D.; Duchemin, I.; Blase, X. Benchmarking the Bethe-Salpeter Formalism on a Standard Organic Molecular Set. *J. Chem. Theory Comput.* **2015**, *11*, 3290−3304.
(32) Jacquemin, D.; Duchemin, I.; Blondel, A.; Blase, X. Assessment of the Accuracy of the Bethe-Salpeter (BSE/GW) Oscillator Strengths. *J. Chem. Theory Comput.* **2016**, *12*, 3969−3981.
(33) Jacquemin, D.; Duchemin, I.; Blondel, A.; Blase, X. Benchmark of Bethe-Salpeter for Triplet Excited-States. *J. Chem. Theory Comput.* **2017**, *13*, 767−783.
(34) Liu, X.; Subotnik, J. E. The Variationally Orbital-Adapted Configuration Interaction Singles (VOA-CIS) Approach to Electronically Excited States. *J. Chem. Theory Comput.* **2014**, *10*, 1004−1020.
(35) Silva-Junior, M. R.; Thiel, W. Benchmark of Electronically Excited States for Semiempirical Methods: MNDO, AM1, PM3, OM1, OM2, OM3, INDO/S, and INDO/S2. *J. Chem. Theory Comput.* **2010**, *6*, 1546−1564.
(36) Gadaczek, I.; Krause, K.; Hintze, K. J.; Bredow, T. MSINDO-sCIS: A New Method for the Calculation of Excited States of Large Molecules. *J. Chem. Theory Comput.* **2011**, *7*, 3675−3685.
(37) Sauer, S. P.; Pitzner-Frydendahl, H. F.; Buse, M.; Jensen, H. J. A.; Thiel, W. Performance of SOPPA-based methods in the calculation of vertical excitation energies and oscillator strengths. *Mol. Phys.* **2015**, *113*, 2026−2045.
(38) Harbach, P. H. P.; Wormit, M.; Dreuw, A. The third-order algebraic diagrammatic construction method (ADC(3)) for the polarization propagator for closed-shell molecules: Efficient implementation and benchmarking. *J. Chem. Phys.* **2014**, *141*, 064113.
(39) Helmich, B.; Hättig, C. A pair natural orbital based implementation of ADC(2)-x: Perspectives and challenges for response methods for singly and doubly excited states in large molecules. *Comput. Theor. Chem.* **2014**, *1040-1041*, 35−44.
(40) Winter, N. O. C.; Hättig, C. Scaled opposite-spin CC2 for ground and excited states with fourth order scaling computational costs. *J. Chem. Phys.* **2011**, *134*, 184101.
(41) Sekino, H.; Bartlett, R. J. A linear response, coupled-cluster theory for excitation-energy. *Int. J. Quantum Chem.* **1984**, *26*, 255−265.
(42) Stanton, J. F.; Bartlett, R. J. The equation of motion coupled-cluster method - a systematic biorthogonal approach to molecular-excitation energies, transition-probabilities, and excited-state properties. *J. Chem. Phys.* **1993**, *98*, 7029−7039.
(43) Kánnár, D.; Szalay, P. G. Benchmarking Coupled Cluster Methods on Valence Singlet Excited States. *J. Chem. Theory Comput.* **2014**, *10*, 3757−3765.
(44) Piecuch, P.; Hansen, J. A.; Ajala, A. O. Benchmarking the completely renormalised equation-of-motion coupled-cluster approaches for vertical excitation energies. *Mol. Phys.* **2015**, *113*, 3085−3127.
(45) Nooijen, M.; Bartlett, R. J. A new method for excited states: Similarity transformed equation-of-motion coupled-cluster theory. *J. Chem. Phys.* **1997**, *106*, 6441−6448.
(46) Nooijen, M.; Bartlett, R. J. Similarity transformed equation-of-motion coupled-cluster theory: Details, examples, and comparisons. *J. Chem. Phys.* **1997**, *107*, 6812−6830.
(47) Nooijen, M.; Lotrich, V. Extended similarity transformed equation-of-motion coupled cluster theory (extended-STEOM-CC): Applications to doubly excited states and transition metal compounds. *J. Chem. Phys.* **2000**, *113*, 494−507.
(48) Sous, J.; Goel, P.; Nooijen, M. Similarity transformed equation of motion coupled cluster theory revisited: a benchmark study of valence excited states. *Mol. Phys.* **2014**, *112*, 616−638.
(49) Dutta, A. K.; Nooijen, M.; Neese, F.; Izsák, R. Exploring the Accuracy of a Low Scaling Similarity Transformed Equation of Motion Method for Vertical Excitation Energies. *J. Chem. Theory Comput.* **2018**, *14*, 72−91.
(50) Helmich, B.; Hättig, C. Local pair natural orbitals for excited states. *J. Chem. Phys.* **2011**, *135*, 214106.
(51) Helmich, B.; Hättig, C. A pair natural orbital implementation of the coupled cluster model CC2 for excitation energies. *J. Chem. Phys.* **2013**, *139*, 084114.
(52) Frank, M. S.; Hättig, C. A pair natural orbital based implementation of CCSD excitation energies within the framework of linear response theory. *J. Chem. Phys.* **2018**, *148*, 134102.
(53) Dutta, A. K.; Neese, F.; Izsák, R. Towards a pair natural orbital coupled cluster method for excited states. *J. Chem. Phys.* **2016**, *145*, 034102.
(54) Peng, C.; Clement, M. C.; Valeev, E. F. State-Averaged Pair Natural Orbitals for Excited States: A Route toward Efficient Equation of Motion Coupled-Cluster. *J. Chem. Theory Comput.* **2018**, *14*, 5597−5607.

DOI: 10.1021/acs.jctc.9b00325
J. Chem. Theory Comput. 2019, 15, 4170−4179

(55) Schapiro, I.; Sivalingam, K.; Neese, F. Assessment of n-Electron Valence State Perturbation Theory for Vertical Excitation Energies. *J. Chem. Theory Comput.* **2013**, *9*, 3567−3580.
(56) Hubert, M.; Hedegård, E. D.; Jensen, H. J. A. Investigation of Multiconfigurational Short-Range Density Functional Theory for Electronic Excitations in Organic Molecules. *J. Chem. Theory Comput.* **2016**, *12*, 2203−2213.
(57) Hedegård, E. D. Assessment of oscillator strengths with multiconfigurational short-range density functional theory for electronic excitations in organic molecules. *Mol. Phys.* **2017**, *115*, 26−38.
(58) Sharkas, K.; Savin, A.; Jensen, H. J. A.; Toulouse, J. A multiconfigurational hybrid density-functional theory. *J. Chem. Phys.* **2012**, *137*, 044104.
(59) Fromager, E.; Knecht, S.; Jensen, H. J. A. Multi-configuration time-dependent density-functional theory based on range separation. *J. Chem. Phys.* **2013**, *138*, 084101.
(60) Hedegård, E. D.; Toulouse, J.; Jensen, H. J. A. Multiconfigurational short-range density-functional theory for open-shell systems. *J. Chem. Phys.* **2018**, *148*, 214103.
(61) Dalgaard, E. Time-dependent multiconfigurational Hartree-Fock theory. *J. Chem. Phys.* **1980**, *72*, 816−823.
(62) Olsen, J.; Jørgensen, P. Linear and nonlinear response functions for an exact state and for an MCSCF state. *J. Chem. Phys.* **1985**, *82*, 3235−3264.
(63) Olsen, J.; Jørgensen, P. *Modern Electronic Structure Theory*; World Scientific: Singapore, 1995; pp 857−990.
(64) Yeager, D. L.; Jørgensen, P. A multiconfigurational time-dependent Hartree−Fock approach. *Chem. Phys. Lett.* **1979**, *65*, 77−80.
(65) Docken, K. K.; Hinze, J. LiH Potential Curves and Wavefunctions for $X\ ^1\Sigma^+$, $A\ ^1\Sigma^+$, $B\ ^1\Pi$, $^3\Sigma^+$, and $^3\Pi$. *J. Chem. Phys.* **1972**, *57*, 4928−4936.
(66) Werner, H.-J.; Meyer, W. A quadratically convergent MCSCF method for the simultaneous optimization of several states. *J. Chem. Phys.* **1981**, *74*, 5794−5801.
(67) Booth, G. H.; Thom, A. J. W.; Alavi, A. Fermion Monte Carlo without fixed nodes: A game of life, death, and annihilation in Slater determinant space. *J. Chem. Phys.* **2009**, *131*, 054106.
(68) Thomas, R. E.; Sun, Q.; Alavi, A.; Booth, G. H. Stochastic Multiconfigurational Self-Consistent Field Theory. *J. Chem. Theory Comput.* **2015**, *11*, 5316−5325.
(69) Huron, B.; Malrieu, J. P.; Rancurel, P. Iterative perturbation calculations of ground and excited state energies from multiconfigurational zeroth-order wavefunctions. *J. Chem. Phys.* **1973**, *58*, 5745−5759.
(70) Holmes, A. A.; Tubman, N. M.; Umrigar, C. J. Heat-Bath Configuration Interaction: An Efficient Selected Configuration Interaction Algorithm Inspired by Heat-Bath Sampling. *J. Chem. Theory Comput.* **2016**, *12*, 3674−3680.
(71) Zimmerman, P. M. Strong correlation in incremental full configuration interaction. *J. Chem. Phys.* **2017**, *146*, 224104.
(72) Eriksen, J. J.; Lipparini, F.; Gauss, J. Virtual Orbital Many-Body Expansions: A Possible Route towards the Full Configuration Interaction Limit. *J. Phys. Chem. Lett.* **2017**, *8*, 4633−4639.
(73) Mussard, B.; Sharma, S. One-Step Treatment of Spin-Orbit Coupling and Electron Correlation in Large Active Spaces. *J. Chem. Theory Comput.* **2018**, *14*, 154−165.
(74) Chakraborty, R.; Ghosh, P.; Ghosh, D. Evolutionary algorithm based configuration interaction approach. *Int. J. Quantum Chem.* **2018**, *118*, No. e25509.
(75) White, S. R. Density matrix formulation for quantum renormalization groups. *Phys. Rev. Lett.* **1992**, *69*, 2863−2866.
(76) White, S. R. Density-matrix algorithms for quantum renormalization groups. *Phys. Rev. B: Condens. Matter Mater. Phys.* **1993**, *48*, 10345−10356.
(77) Zgid, D.; Nooijen, M. The density matrix renormalization group self-consistent field method: Orbital optimization with the density matrix renormalization group method in the active space. *J. Chem. Phys.* **2008**, *128*, 144116.
(78) Ghosh, D.; Hachmann, J.; Yanai, T.; Chan, G. K.-L. Orbital optimization in the density matrix renormalization group, with applications to polyenes and β-carotene. *J. Chem. Phys.* **2008**, *128*, 144117.
(79) Yanai, T.; Kurashige, Y.; Ghosh, D.; Chan, G. K.-L. Accelerating convergence in iterative solution for large-scale complete active space self-consistent-field calculations. *Int. J. Quantum Chem.* **2009**, *109*, 2178−2190.
(80) Wouters, S.; Poelmans, W.; Ayers, P. W.; Van Neck, D. CheMPS2: A free open-source spin-adapted implementation of the density matrix renormalization group for ab initio quantum chemistry. *Comput. Phys. Commun.* **2014**, *185*, 1501−1514.
(81) Wouters, S.; Poelmans, W.; De Baerdemacker, S.; Ayers, P. W.; Van Neck, D. CheMPS2: Improved DMRG-SCF routine and correlation functions. *Comput. Phys. Commun.* **2015**, *191*, 235−237.
(82) Szalay, S.; Pfeffer, M.; Murg, V.; Barcza, G.; Verstraete, F.; Schneider, R.; Legeza, Ö. Tensor product methods and entanglement optimization for ab initio quantum chemistry. *Int. J. Quantum Chem.* **2015**, *115*, 1342−1391.
(83) Ma, Y.; Knecht, S.; Keller, S.; Reiher, M. Second-Order Self-Consistent-Field Density-Matrix Renormalization Group. *J. Chem. Theory Comput.* **2017**, *13*, 2533−2549.
(84) Li Manni, G.; Smart, S. D.; Alavi, A. Combining the Complete Active Space Self-Consistent Field Method and the Full Configuration Interaction Quantum Monte Carlo within a Super-CI Framework, with Application to Challenging Metal-Porphyrins. *J. Chem. Theory Comput.* **2016**, *12*, 1245−1258.
(85) Angeli, C.; Borini, S.; Cestari, M.; Cimiraglia, R. A quasidegenerate formulation of the second order n-electron valence state perturbation theory approach. *J. Chem. Phys.* **2004**, *121*, 4043−4049.
(86) Granovsky, A. A. Extended multi-configuration quasi-degenerate perturbation theory: The new approach to multi-state multi-reference perturbation theory. *J. Chem. Phys.* **2011**, *134*, 214113.
(87) Shiozaki, T.; Győrffy, W.; Celani, P.; Werner, H.-J. Communication: Extended multi-state complete active space second-order perturbation theory: Energy and nuclear gradients. *J. Chem. Phys.* **2011**, *135*, 081106.
(88) Aoto, Y. A.; Köhn, A. Internally contracted multireference coupled-cluster theory in a multistate framework. *J. Chem. Phys.* **2016**, *144*, 074103.
(89) Jørgensen, P.; Simons, J. *Second Quantization-Based Methods in Quantum Chemistry*; Academic Press, Inc., 1981.
(90) Oddershede, J.; Jørgensen, P.; Yeager, D. L. Polarization propagator methods in atomic and molecular calculations. *Comput. Phys. Rep.* **1984**, *2*, 33−92.
(91) Helmich-Paris, B. CASSCF linear response calculations for large open-shell molecules. *J. Chem. Phys.* **2019**, *150*, 174121.
(92) Loos, P.-F.; Scemama, A.; Blondel, A.; Garniron, Y.; Caffarel, M.; Jacquemin, D. A Mountaineering Strategy to Excited States: Highly Accurate Reference Energies and Benchmarks. *J. Chem. Theory Comput.* **2018**, *14*, 4360−4379.
(93) Li, Z.; Liu, W. Critical Assessment of TD-DFT for Excited States of Open-Shell Systems: I. Doublet-Doublet Transitions. *J. Chem. Theory Comput.* **2016**, *12*, 238−260.
(94) Suo, B.; Shen, K.; Li, Z.; Liu, W. Performance of TD-DFT for Excited States of Open-Shell Transition Metal Compounds. *J. Phys. Chem. A* **2017**, *121*, 3929−3942.
(95) Loos, P.-F.; Jacquemin, D. Chemically Accurate 0−0 Energies with Not-so-Accurate Excited State Geometries. *J. Chem. Theory Comput.* **2019**, *15*, 2481−2491.
(96) Kollmar, C.; Sivalingam, K.; Helmich-Paris, B.; Angeli, C.; Neese, F. A perturbation-based super-CI approach for the orbital optimization of a CASSCF wave function. *J. Comput. Chem.* **2019**, *40*, 1463−1470.
(97) Neese, F. The ORCA program system. *WIREs Comput. Mol. Sci.* **2012**, *2*, 73−78.

DOI: 10.1021/acs.jctc.9b00325
J. Chem. Theory Comput. 2019, 15, 4170−4179

(98) Schäfer, A.; Huber, C.; Ahlrichs, R. Fully optimized contracted Gaussian basis sets of triple zeta valence quality for atoms Li to Kr. *J. Chem. Phys.* **1994**, *100*, 5829−5835.
(99) Kendall, R. A.; Dunning, T. H.; Harrison, R. J. Electron-affinities of the 1st-row atoms revisited - systematic basis-sets and wave-functions. *J. Chem. Phys.* **1992**, *96*, 6796−6806.
(100) Weigend, F. Hartree-Fock exchange fitting basis sets for H and Rn. *J. Comput. Chem.* **2008**, *29*, 167−175.
(101) Weigend, F.; Köhn, A.; Hättig, C. Efficient use of the correlation consistent basis sets in resolution of the identity MP2 calculations. *J. Chem. Phys.* **2002**, *116*, 3175−3183.
(102) Vahtras, O.; Almlöf, J.; Feyereisen, M. W. Integral approximations for LCAO-SCF calculations. *Chem. Phys. Lett.* **1993**, *213*, 514−518.
(103) Martin, R. L. Natural transition orbitals. *J. Chem. Phys.* **2003**, *118*, 4775−4777.
(104) Sokolov, A. Y. Multi-reference algebraic diagrammatic construction theory for excited states: General formulation and first-order implementation. *J. Chem. Phys.* **2018**, *149*, 204113.
(105) Samanta, P. K.; Mukherjee, D.; Hanauer, M.; Köhn, A. Excited states with internally contracted multireference coupled-cluster linear response theory. *J. Chem. Phys.* **2014**, *140*, 134108.
(106) Malmqvist, P.-Å.; Roos, B. O. The CASSCF state interaction method. *Chem. Phys. Lett.* **1989**, *155*, 189−194.
(107) Li, C.; Verma, P.; Hannon, K. P.; Evangelista, F. A. A low-cost approach to electronic excitation energies based on the driven similarity renormalization group. *J. Chem. Phys.* **2017**, *147*, 074107.

DOI: 10.1021/acs.jctc.9b00325
J. Chem. Theory Comput. 2019, 15, 4170−4179